

See discussions, stats, and author profiles for this publication at: <https://www.researchgate.net/publication/258683637>

Block Random Copolymers of N-Alkyl-Substituted Acrylamides with Double Thermosensitivity

ARTICLE in MACROMOLECULES · FEBRUARY 2012

Impact Factor: 5.8 · DOI: 10.1021/ma2027269

CITATIONS

13

READS

59

3 AUTHORS:



Mohammad T. Savoji

University of Minnesota Twin Cities

9 PUBLICATIONS 45 CITATIONS

SEE PROFILE



Satu Strandman

Université de Montréal

32 PUBLICATIONS 469 CITATIONS

SEE PROFILE



X. X. Zhu

Université de Montréal

234 PUBLICATIONS 5,016 CITATIONS

SEE PROFILE

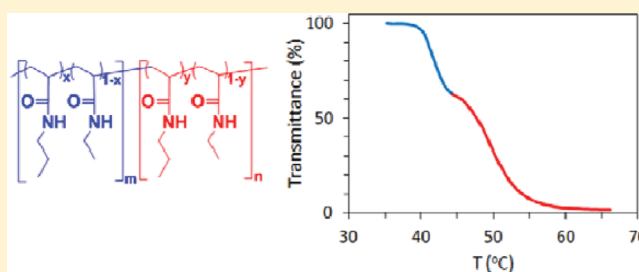
Block Random Copolymers of *N*-Alkyl-Substituted Acrylamides with Double Thermosensitivity

Mohammad T. Savoji, Satu Strandman, and X. X. Zhu*

Department of Chemistry, Université de Montréal, CP 6128, Succursale Centre-ville, Montreal, QC H3C 3J7, Canada

S Supporting Information

ABSTRACT: Block copolymers consisting of two segments of random copolymers of *N*-alkylacrylamides have been synthesized by a sequential reversible addition–fragmentation chain transfer (RAFT) polymerization. The copolymers in the form of $A_nB_m-b-A_pB_q$ have been made of two blocks of *N*-*n*-propylacrylamide (nPA) and *N*-ethylacrylamide (EA) of different compositions to obtain polymers with stepwise thermosensitivity. The control of the RAFT polymerization was confirmed by studying the kinetics of the copolymerization process. The block random copolymer, poly($nPA_x-co-EA_{1-x}$)-*block*-poly($nPA_y-co-EA_{1-y}$), is well-defined and has a low polydispersity. The cloud points of the random copolymers can be tuned by varying the chemical composition of the copolymers. The diblock copolymer exhibited a two-step phase transition upon heating to 41.5 and 53.0 °C, corresponding to the cloud points of the individual blocks. Dynamic light scattering experiments also showed the stepwise aggregation properties of the copolymer in aqueous solutions.



INTRODUCTION

Thermoresponsive polymers have been widely investigated for their potential in biomedical applications.^{1–4} Many polymers based on *N*-alkyl-substituted acrylamides, the most well-known of which being poly(*N*-isopropylacrylamide), exhibit a lower critical solution temperature (LCST) in water.⁵ The thermoresponsiveness of these polymers depends on the relative hydrophobicity or hydrophilicity of the *N*-alkylacrylamide monomers,^{5,6} in addition to the effects of molar mass, concentrations, and additives. Increased hydrophobicity of the substitution groups leads to a lower phase transition temperature of the polymers obtained.^{7–10} The cloud points (CPs) of the polymers can be tuned by the varying the chemical composition of the random copolymers based on *N*-alkyl-substituted (meth)acrylamides.^{11–13} Diblock copolymers with dual thermoresponsive behavior have been synthesized by the incorporation of blocks with different cloud points.^{4,14–19} We have made various di- and triblock copolymers of *N*-alkylacrylamides and showed that they exhibited multiple CPs in aqueous solutions,^{20,21} corresponding to different stages of their aggregation.^{22,23} The phase transitions are usually accompanied by changes in the micellar size or shape and solution properties. However, the choice of the substitution groups on such monomers limits the range of the phase transition temperatures. To tailor the properties of the materials, it would be ideal to have blocks available with a thermosensitivity at any desired temperature. This may be achieved by varying the chemical composition of a random copolymer.¹² Therefore, our approach is to make a block copolymer of two random copolymer sequences with different thermosensitivities. We choose to use the reversible addition–

fragmentation chain transfer (RAFT) polymerization method^{24,25} to grow two block of random copolymers of *N*-*n*-propylacrylamide (nPA) and *N*-ethylacrylamide (EA) with compositions adjusted for the desired transition temperatures. We report here the design, synthesis, and characterization of a diblock thermoresponsive copolymer with two distinct transition temperatures corresponding to the two random copolymers synthesized by sequential RAFT copolymerization.

EXPERIMENTAL SECTION

Materials. 2,2'-Azobis(isobutyronitrile) (AIBN) from Eastman Kodak was recrystallized from methanol and stored in dark bottles in a refrigerator. Acryloyl chloride, ethylamine, and *n*-propylamine were purchased from Aldrich and were used without further purification. *N*-*n*-Propylacrylamide (nPA) and *N*-ethylacrylamide (EA) were prepared by reacting acryloyl chloride with the corresponding alkylamines following a reported procedure.²⁶ 2-Dodecylsulfanythiocarbonylsulfanyl-2-methylpropionic acid (DMP) was used as a highly efficient chain transfer reagent (CTA) and prepared according to the procedure reported by Lai et al.²⁷ Water was purified using a Millipore Milli-Q system. Anhydrous and oxygen-free dioxane was obtained by passage through columns packed with activated alumina and supported copper catalyst (Glass Contour, Irvine, CA).

Polymer Synthesis. The monomers nPA and EA were added at a predetermined ratio along with trithiocarbonate DMP as the CTA and AIBN as the initiator in a 100 mL Schlenk tube equipped with a magnetic stirrer bar. A fixed volume of anhydrous dioxane was then transferred to the Schlenk tube. The ratio of [monomers]:[DMP]:

Received: December 16, 2011

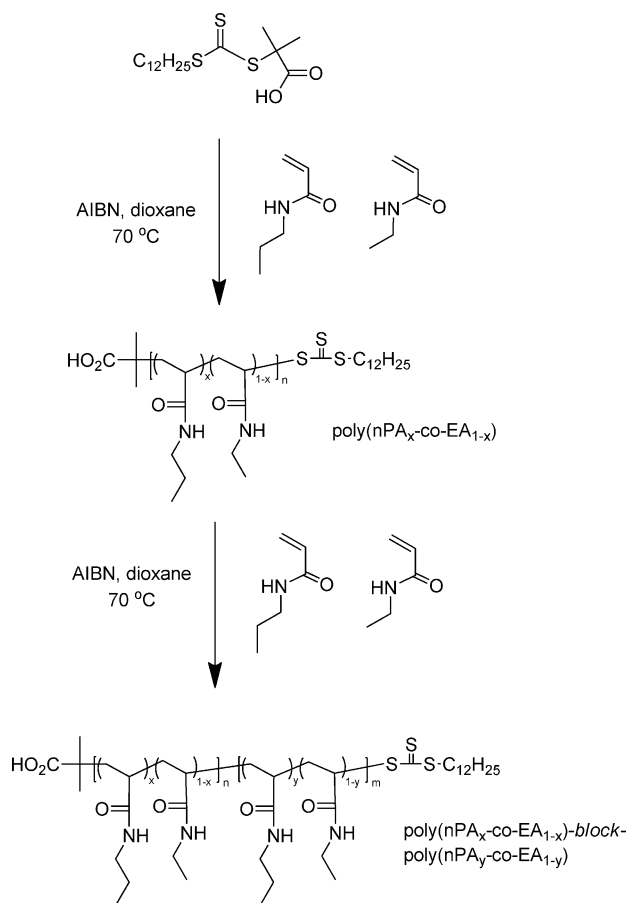
Revised: January 24, 2012

Published: February 8, 2012



[AIBN] was fixed at 200:1:0.1, and the total monomer concentration was 0.3 g/mL. The mixture was degassed by three freeze–pump–thaw cycles prior to immersing it in a preheated oil bath. The reaction temperature was set to 70 °C, and the reaction was conducted for 90 min before terminating it by exposing the reaction mixture to air and immersing it in an ice bath. The product was then precipitated in diethyl ether, filtered, and dried in vacuum oven at 60 °C to yield poly($n\text{PA}_x\text{-co-EA}_{1-x}$)-CTA as a yellowish powder. The resulting random copolymer was then used as the DMP-ended macro-CTA in the second step to make a diblock copolymer using the reactant ratio [monomer]:[macro-CTA]:[AIBN] of 400:1:0.1. The procedure for diblock copolymerization was the same as for random copolymeriza-

Scheme 1. RAFT Copolymerization of nPA and EA for the Preparation of Poly($n\text{PA}_x\text{-co-EA}_{1-x}$) and Further Chain Extension Leading to a Diblock Random Copolymer Poly($n\text{PA}_x\text{-co-EA}_{1-x}$)-block-poly($n\text{PA}_y\text{-co-EA}_{1-y}$)



tion, except that DMP has been replaced by macro-CTA (Scheme 1). In the kinetic studies, aliquots of the reaction mixture were withdrawn during the course of the copolymerization and analyzed by size exclusion chromatography (SEC) and nuclear magnetic resonance (NMR) spectroscopy.

Polymer Characterization. Molar masses and polydispersity indices (PDI) of the polymers were obtained by SEC on a Waters 1525 system equipped with three Waters Styragel columns and a refractive index detector (Waters 2410) at 35 °C. N,N -Dimethylformamide (DMF) was employed as the mobile phase at a flow rate of 1 mL/min, and the system was calibrated by poly(methyl methacrylate) standards. In kinetic studies, the volatile species were removed in a vacuum oven at 60 °C from the samples taken at different time intervals during the course of the reaction.

The NMR spectra of the monomers and polymers in deuterated chloroform (CDCl_3) were determined on a Bruker AV-400 spectrometer operating at 400 MHz for protons. The chemical shifts are given in reference to the solvent peak at 7.26 ppm. The theoretical molar masses were calculated from the conversions given by ^1H NMR according to

$$\bar{M}_{n,\text{th}} = M_{\text{CTA}} + \frac{[\text{monomer}]}{[\text{CTA}]} \times M_{\text{monomer}} \times \text{conversion} \quad (1)$$

where M_{CTA} is the molar mass of the chain transfer agent and [monomer] and [CTA] are the initial monomer and CTA concentrations, respectively. M_{monomer} is the weighted molar mass of the comonomers and calculated from the molar ratios of comonomers in the product obtained by ^1H NMR. The molar masses of the polymers were not determined by ^1H NMR because of the overlap of the methyl group signals from EA and from DMP end group at 0.99 ppm. For a block copolymer, [CTA] in eq 1 is replaced by the concentration of macro-CTA.

The CPs of the polymers were determined from the optical transmittance measured on a Cary 300 Bio UV–vis spectrophotometer equipped with a temperature-controlled sample holder. Samples were prepared by the dissolution of copolymers in distilled water in an ice–water bath, after which the solutions were homogenized by ultrasonication. The absorbance was measured at different wavelengths for the aqueous solution of polymers 1.0 mg/mL by continuous heating at rate of 0.1 °C/min over various temperature ranges or stepwise heating at 1 °C intervals with 20 min equilibration at each temperature, which was also the heating procedure used in the light scattering experiments where continuous heating was not possible. Here, the CP is defined as a temperature at which the differential of transmittance change with respect to the temperature at a certain wavelength is maximal.²⁸ Another definition is the temperature corresponding to a 10% or 50% reduction in the initial transmittance.^{20,25,29} For individual blocks, the temperature at which 50% transmittance was lost upon heating was considered as the CP. For block copolymers, the CP is determined from the middle point between the onset and the offset of the transmittance curve as a function of temperature.

Dynamic light scattering (DLS) studies on the temperature-dependent aggregation behavior were carried out on a CGS-3 compact goniometer (ALV GmbH) equipped with an ALV-5000 multi tau digital real time correlator at chosen temperatures using a Science/Electronics temperature controller. The laser wavelength was 632 nm, and the scattering angle was fixed at 90°. All solutions were made with the concentration of 2.0 mg/mL and filtered through 0.22 μm Millipore filters to remove dust. The samples were heated at 1 °C intervals within 20 min equilibration time. The results were analyzed by CONTIN inverse Laplace transform algorithm. The decay rate distributions were transformed to an apparent diffusion coefficient and the apparent intensity-weighted hydrodynamic diameters of the polymers was obtained from the Stokes–Einstein equation.

RESULTS AND DISCUSSION

Kinetics of the RAFT Copolymerization of N -Alkyl-Substituted Acrylamides. N - n -Propylacrylamide and N -ethylacrylamide were copolymerized in dioxane at 70 °C using a monomer ratio of 70:30 ($n\text{PA}$:EA) and a reactant ratio of [monomers]:[CTA]:[initiator] of 200:1:0.1. The conversion was monitored by ^1H NMR spectroscopy of the samples withdrawn from the reaction mixture at regular time intervals and determined by comparing the integrated areas of the characteristic proton signals from the vinyl group of monomers in the region of 5.5–6.3 ppm with the integrated areas of the methyl signals of the polymer at 0.8–1.2 ppm (Figure S1, Supporting Information). Of course, the contribution of residual methyl group signals is subtracted from the total

integration in the region of 0.8–1.2 ppm (as explained in Figure S2).

The composition of the copolymer remained constant throughout the duration of the polymerization process as verified by ^1H NMR (Figure S2), which indicates the random nature of the copolymerization. The evolution of the molar mass with conversion is presented in Figure 1. The increase in

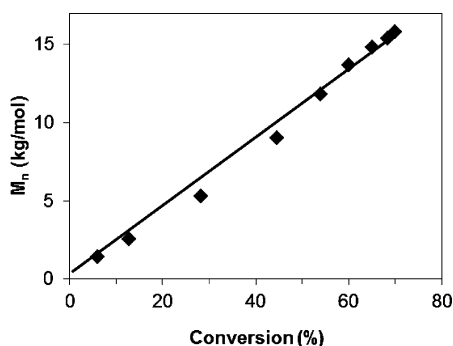


Figure 1. Number-average molar mass M_n as a function of conversion of the monomers for the RAFT copolymerization of nPA and EA at monomer ratio of 70:30 (nPA:EA). Solid line represents the theoretical molar masses calculated from eq 1.

molar mass follows the theoretical line up to 70% conversion, which shows the controlled character of the copolymerization. An increase in polydispersity is observed at higher conversions (Figure 2A) and a negative deviation from linearity in the

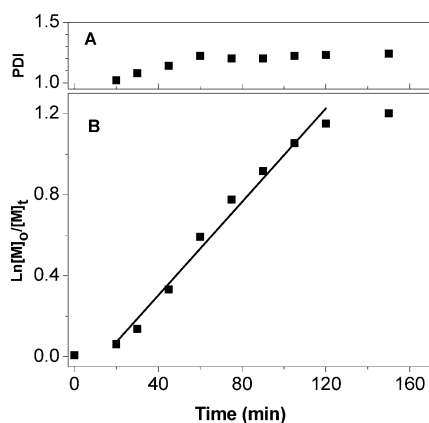


Figure 2. (A) Polydispersity index (PDI) and (B) semilogarithmic kinetic plot of the monomer conversion $\ln([M]_0/[M]_t)$ as a function of reaction time for the RAFT copolymerization of nPA and EA in dioxane at 70 °C with a monomer ratio [nPA]:[EA] of 70:30 and [monomers]:[CTA]:[initiator] ratio of 200:1:0.1. Solid line is a linear fit to part of the data to serve as a visual guide.

pseudo-first-order plot (Figure 2B) occurred after 120 min reaction time, both frequently reported for the RAFT polymerization of *N*-substituted acrylamides.^{20,25,30–32} An inhibition period of ~15 min at the beginning of polymerization is attributed to the slow fragmentation of CTA.^{33–36} The kinetic data indicate that the concentration of the radical species is constant during the reaction, and thus, the polymerization is controlled in this range of conversions. The SEC chromatograms of the samples withdrawn at different reaction times (Figure S3) show that the higher polydispersities at high conversions arise from low-molar-mass tailing similar to

our earlier observations²⁰ as well as those by other groups.^{30,35,37}

In our earlier discussion, we showed that the negative deviation of the kinetic plot may not arise from the initiator-derived radicals but is rather related to the number of other radicals, which can be corrected to some degree by lowering the polymerization temperature.²⁰ This was our motivation for the choice of current reaction temperature (70 °C). The reactivities of *N*-alkylacrylamides are also known to depend on their structure, the polymerizations of *N,N*-dialkyl-substituted acrylamides being faster and more controlled than those of their monosubstituted counterparts with less negative deviation in the kinetic behavior.²⁰ In comparison with our earlier kinetic data on the homopolymerization of nPA with the same [CTA]:[initiator] ratio at the same temperature,²⁰ the copolymerization of nPA and EA shows better linearity up to higher conversions. Other monomers (*N*-*tert*-butylacrylamide, tBA, and *N,N*-dimethylacrylamide, DMA) with different mole fractions were also copolymerized under the same conditions, and they showed the same kinetic behavior as P(nPA_{0.7}EA_{0.3}) (data not shown). On the basis of the kinetic data, the reaction conditions are chosen to provide an active macro-CTA that can be employed in the subsequent block copolymerization.

CPs of the Random Copolymers. Various *N*-alkyl-substituted acrylamide homopolymers and corresponding random copolymers were synthesized and studied in our group.¹² Among them, *N*-*n*-propylacrylamide (nPA) and *N*-ethylacrylamide (EA) were selected for the current study. These monomers have different hydrophilicities and thus the corresponding copolymers have different CPs. A series of copolymers with different nPA:EA ratios were synthesized, and their thermoresponsiveness was tested in aqueous solutions. Table 1 shows the characteristics of the copolymers. The

Table 1. Chemical Compositions and CP of Poly(nPA_{*x*}-co-EA_{1-*x*}) Copolymers with Different Ratios of the Comonomers

polymer	M_n^a (g/mol)	PDI ^a	nPA:EA ratio in final polymer ^b	CP (°C) ^c
PEA	19 800	1.08	100:0	>85
P(nPA _{0.2} EA _{0.8})	15 200	1.24	19.1:80.9	75
P(nPA _{0.4} EA _{0.6})	19 800	1.13	40.5:59.5	52
P(nPA _{0.5} EA _{0.5})	12 000	1.18	49.8:50.2	45
P(nPA _{0.6} EA _{0.4})	20 100	1.23	58.2:41.8	40
P(nPA _{0.7} EA _{0.3})	13 200	1.11	69.9:30.1	37
P(nPA _{0.8} EA _{0.2})	16 500	1.21	78.1:21.9	33
PnPA	12 800	1.10	0:100	20

^aDetermined by SEC. ^bDetermined by ^1H NMR. ^cDetermined by UV–vis spectroscopy at $\lambda = 350$ nm.

copolymer compositions are nearly identical to the feed ratios, supporting our earlier observations on the similar reactivity of *N*-alkylacrylamides¹² and suggesting that the copolymers are statistically random.

Figure 3 shows the CPs of poly(nPA_{*x*}-co-EA_{1-*x*}) random copolymers as a function of the mole fraction of EA in the random copolymer. The CP increases with an increase in the mole fraction of the more hydrophilic monomer EA and follows eq 2 as a function of the comonomer composition:¹²

$$T = \frac{\mu_1 T_1 + k \mu_2 T_2}{\mu_1 + k \mu_2} \quad (2)$$

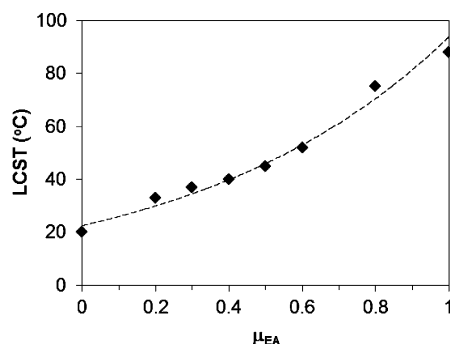


Figure 3. CPs of poly($n\text{PA}_x\text{-co-EA}_{1-x}$) aqueous solution as a function of the mole fraction of EA, μ_{EA} . The dashed line shows the curve fitting to eq 2, yielding a k value of 0.69.

where T , T_1 , and T_2 are the CPs of the random copolymer, PEA, and PnPA, respectively. μ_1 and μ_2 are the mole fractions of EA and nPA (note that $\mu_1 = 1 - \mu_2$), respectively, and k is a weighting parameter which can be deduced from curve fitting to the experimental data. A k value of 1 would be obtained in the case of a linear relationship of T vs μ_1 . In the current case, the plot has a concave shape, yielding a k value of 0.69. In comparison, a k value of 0.51 was observed for the copolymers of EA and a more hydrophobic monomer, *N-tert*-butylacrylamide (tBA).¹² Figure 3 shows a 15 °C difference between the CPs of P($n\text{PA}_{0.4}\text{EA}_{0.6}$) and P($n\text{PA}_{0.7}\text{EA}_{0.3}$), enough to distinguish the phase transitions in a block copolymer. Therefore, these monomer ratios were chosen to build the two blocks of the copolymer.

Preparation of a Diblock Random Copolymer by RAFT Polymerization. A random copolymer of nPA and EA with a comonomer ratio of 70:30, P($n\text{PA}_{0.7}\text{EA}_{0.3}$), was synthesized to serve as a macro-CTA (macro-chain transfer agent) for the chain extension. The polymerization was stopped at 60% conversion to avoid the formation of dead chain ends. The polymer was purified by a precipitation in diethyl ether prior to the addition of the second block so that it was free of monomers as shown by ^1H NMR spectroscopy (Figure S1, Supporting Information). The details of the macro-CTA copolymer are presented in Table 2.

Table 2. Conversions and the Compositions of Mono- and Diblock Random Copolymers

polymer	nPA:EA ratio in the blocks ^a	conv ^a (%)	M_n		PDI ^c
			theor ^b	SEC ^c	
P($n\text{PA}_{0.7}\text{EA}_{0.3}$)	69.9:30.1	60	13 500	13 200	1.11
P($n\text{PA}_{0.7}\text{EA}_{0.3}$)- <i>b</i> -P($n\text{PA}_{0.4}\text{EA}_{0.6}$)	41.2:58.8	66	41 000	45 000	1.26

^aDetermined by ^1H NMR. ^bCalculated from eq 1. ^cDetermined by SEC.

As mentioned above, the comonomer ratio for building the second block was chosen to yield two separable phase transitions in aqueous solution. The conditions of the block copolymerization of nPA and EA at a feed ratio of 60:40 were the same as in the first copolymerization, but the ratio of reactants [monomer]:[macro-CTA]:[AIBN] was set at 400:1:0.1 to provide a longer second block that would allow a better solubilization of the final block copolymer above the CP of the first block. It is known that some monomers tend to

produce more deactivated macro-CTAs in a RAFT copolymerization than the others. Although this phenomenon is not fully understood, we have earlier shown that macro-CTAs of *N*-monosubstituted acrylamides such as nPA and iPA mostly remain active, more than those of the disubstituted acrylamides.^{20,21}

The results of the block copolymerization are summarized in Table 2, and the SEC chromatograms of the macro-CTA and the resulting block copolymer are shown in Figure 4, indicating

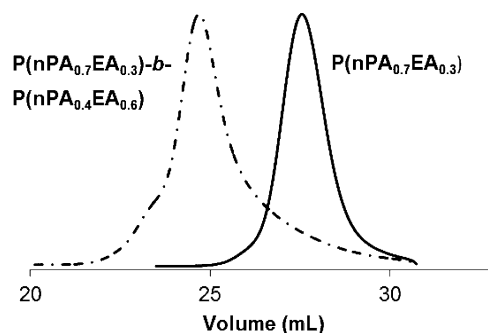


Figure 4. SEC chromatograms of P($n\text{PA}_{0.7}\text{EA}_{0.3}$) (macro-CTA) and P($n\text{PA}_{0.7}\text{EA}_{0.3}$)-*b*-P($n\text{PA}_{0.4}\text{EA}_{0.6}$) (diblock copolymer).

the livingness of block copolymerization. The conversion of the second block was 66%, and the molar mass of the block random copolymer was well in accordance with the theoretical value calculated by eq 1. The polydispersity increased upon block copolymerization, indicating some loss of control over the RAFT polymerization process, commonly observed for macro-CTAs and associated with a small quantity of inactive species in the reaction.³⁸ The monomer composition of the P($n\text{PA}_{0.4}\text{EA}_{0.6}$) block in Table 2 was calculated from the ^1H NMR spectra of macro-CTA and diblock copolymer (Figure S4). On the basis of the molar masses given by SEC and the monomer compositions, the block ratio of the P($n\text{PA}_{0.7}\text{EA}_{0.3}$)-*b*-P($n\text{PA}_{0.4}\text{EA}_{0.6}$) diblock copolymer is 1:2.4.

Solution Properties of Copolymers and Block Random Copolymer. To demonstrate the phase transitions of the individual blocks of P($n\text{PA}_{0.7}\text{EA}_{0.3}$)-*b*-P($n\text{PA}_{0.4}\text{EA}_{0.6}$) diblock random copolymer, the transmittance curves of aqueous solutions of P($n\text{PA}_{0.7}\text{EA}_{0.3}$) and P($n\text{PA}_{0.4}\text{EA}_{0.6}$) at a concentration of 1.0 mg/mL upon heating are shown in Figure 5A, indicating CPs of 37 and 52 °C, respectively. The molar masses of the random copolymers were 13 200 and 19 800 g/mol, respectively (Table 1).

Figure 5B shows two clear shifts in the transmittance of P($n\text{PA}_{0.7}\text{EA}_{0.3}$)-*b*-P($n\text{PA}_{0.4}\text{EA}_{0.6}$) solution with increasing temperature. When observed at 350 nm, the transmittance starts to decrease abruptly at 40 °C as the more hydrophobic P($n\text{PA}_{0.7}\text{EA}_{0.3}$) block becomes insoluble upon heating, the middle point of the first transition being at 41.5 °C. When the temperature continues to rise, the second increase in the turbidity starts at 46 °C with a middle point of the transition at 53 °C, corresponding to the CP of P($n\text{PA}_{0.4}\text{EA}_{0.6}$). The broadening of the phase transition temperatures may be influenced by the mutual and opposite effect of the two individual blocks: The more hydrophilic block drags the CP of the neighboring block to a higher temperature while the more hydrophobic one drags the other block to a lower CP. Fast continuous heating without equilibration led to lower apparent transition temperatures (Figure S5), as it may not allow enough

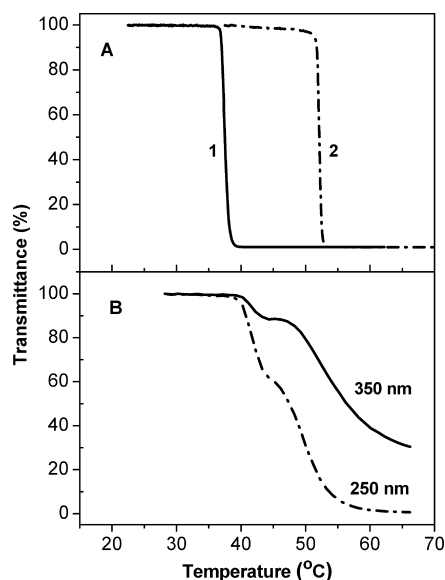


Figure 5. Temperature-dependent transmittance of 1.0 mg/mL aqueous solutions of (A) $P(nPA_{0.7}EA_{0.3})$ and $P(nPA_{0.4}EA_{0.6})$, observed at a wavelength of 350 nm and (B) $P(nPA_{0.7}EA_{0.3})$ - b - $P(nPA_{0.4}EA_{0.6})$ at two wavelengths, 350 and 250 nm. The samples were heated by 1 °C intervals followed by an equilibration for 20 min.

time for the reorganization of individual blocks during the aggregation. The temperature-dependent transmittance of the diblock random copolymer depends on the detection wavelength (Figure S5). It is known that the scattering depends strongly on the wavelength of the light ($\sim \lambda^{-4}$).³⁹ This explains the higher transmittance at 350 nm than at 250 nm since the light of a shorter wavelength is more scattered than that of a longer wavelength. In addition, only the particles larger than the wavelength of light are visible at a certain observation wavelength. Therefore, at longer observation wavelengths, fewer particles are visible, leading to a lower apparent turbidity.²²

The temperature dependence of apparent mean hydrodynamic diameter (D_h) of $P(nPA_{0.7}EA_{0.3})$ - b - $P(nPA_{0.4}EA_{0.6})$ in a 2.0 mg/mL solution is demonstrated in Figure 6, and the

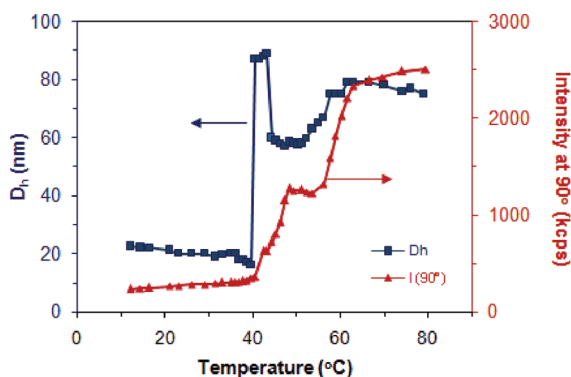
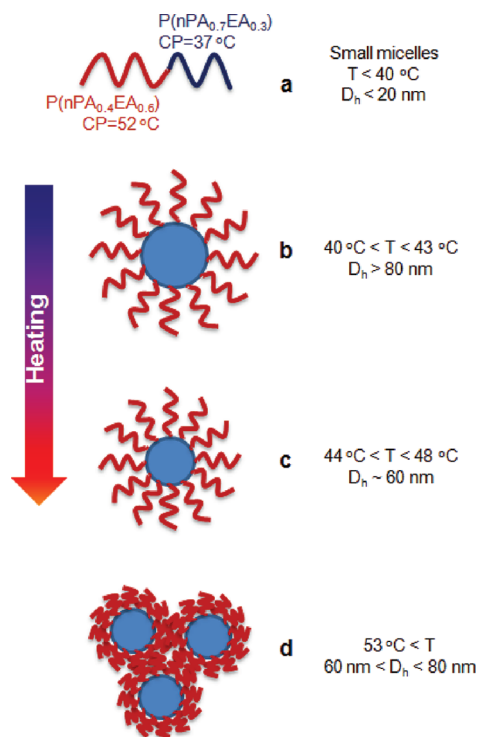


Figure 6. Temperature dependence of mean hydrodynamic diameter (D_h) and scattering intensity obtained by dynamic light scattering at 90° angle for a 2.0 mg/mL aqueous solution of $P(nPA_{0.7}EA_{0.3})$ - b - $P(nPA_{0.4}EA_{0.6})$.

proposed mechanism for the aggregation process is shown in Scheme 2. At low temperatures, the solution consists of small micelles ($D_h \leq 22$ nm) possibly together with molecularly

Scheme 2. Schematic Illustration of the Aggregation Behavior of $P(nPA_{0.7}EA_{0.3})$ - b - $P(nPA_{0.4}EA_{0.6})$ in Water upon Heating: (a) Molecularly Soluble Polymers and Small Micelles below 40 °C; (b) Dehydration of the $P(nPA_{0.7}EA_{0.3})$ Core at 40 °C; (c) Collapsed Aggregates at 44–53 °C; (d) Clusters above 53 °C



dissolved polymers, which compress upon heating prior to reaching the onset of the first CP. Such shrinking has been commonly observed for thermoresponsive polymers due to a coil-to-globule transition.^{40–42} The micellization itself may stem from the hydrophobic $C_{12}H_{25}$ CTA end group of the block copolymer. The micelles start to aggregate when the temperature reaches the onset of the CP transition of the more hydrophobic $P(nPA_{0.7}EA_{0.3})$ block at 40 °C, and the mean diameter suddenly increases as the size distribution becomes bimodal due to the emergence of larger aggregates ($D_h \sim 88$ nm), similar to the observations by Laschewsky and co-workers on triblock copolymers.⁴³ Further heating results in a collapse of the core at 44–48 °C upon the dehydration of the hydrophobic block, after which the aggregated species remain stable. We have earlier described similar aggregation behavior with an initial increase in D_h followed by a collapse for a poly(*N*-*n*-propylacrylamide) homopolymer as well as for its diblock and triblock copolymers.²² At 53 °C, the more hydrophilic $P(nPA_{0.4}EA_{0.6})$ block reaches its CP and becomes more hydrophobic, leading to its contraction in water and further clustering of the micelles. Scattering intensity increases gradually during the aggregation/collapse and clustering processes, with a plateau in between. At 63 °C, the size distribution is monomodal and the mean hydrodynamic diameter of clusters is 79 nm, followed by a small contraction due to further dehydration of the outer block upon heating.

CONCLUSIONS

RAFT polymerization has been successfully used to make random copolymers of *N*-alkyl-substituted acrylamides with

narrow molecular weight distributions. The kinetic study shows the controlled character of the RAFT copolymerization of the two monomers in the family of *N*-alkylacrylamides at conversions below 70%. The CP of the copolymers can be varied over a temperature range of 20–85 °C by adjusting the comonomer ratio, allowing the design of block copolymers of two random copolymers with different phase transition temperatures. The stepwise aggregation of the block copolymer at different temperatures has been clearly shown. While rising the temperature above the CP of the first block leads to clustering and subsequent collapse of the core of the aggregates, heating above the CP of the second block induces further clustering and contraction of the shell through the dehydration of outer block. Further studies by dynamic and static light scattering together with microscopic methods may help to better understand the aggregation process. These block random copolymers expand the scope of thermoresponsive polymers and give promise to novel materials with tailored stimuli-responsive properties.

■ ASSOCIATED CONTENT

■ Supporting Information

¹H NMR spectra of a reaction mixture and of a purified random copolymer, SEC traces of copolymers at different polymerization times, ¹H NMR spectra for the mono- and diblock copolymers, and UV–vis transmittance of the aqueous solution of the polymers at different wavelengths. This material is available free of charge via the Internet at <http://pubs.acs.org>.

■ AUTHOR INFORMATION

Notes

The authors declare no competing financial interest.

■ ACKNOWLEDGMENTS

Financial support from NSERC of Canada, the FQRNT of Quebec, and the Canada Research Chair program is gratefully acknowledged. The authors are members of CSACS funded by FQRNT and GRSTB funded by FRSQ. M.T.S. thanks the Department of Chemistry of Université de Montréal for the Camille Sandorfy Scholarship. The authors thank Prof. F. Winnik and Dr. X. Qiu for their help with the temperature-dependent DLS measurements.

■ REFERENCES

- (1) Li, C.; Madsen, J.; Armes, S. P.; Lewis, A. L. *Angew. Chem., Int. Ed.* **2006**, *45*, 3510–3513.
- (2) Pasparakis, G.; Alexander, C. *Angew. Chem., Int. Ed.* **2008**, *47*, 4847–4850.
- (3) Stuart, M. A. C.; Huck, W. T. S.; Genzer, J.; Muller, M.; Ober, C.; Stamm, M.; Sukhorukov, G. B.; Szleifer, I.; Tsukruk, V. V.; Urban, M.; Winnik, F.; Zauscher, S.; Luzinov, I.; Minko, S. *Nature Mater.* **2010**, *9*, 101–113.
- (4) Jochum, F. D.; Roth, P. J.; Kessler, D.; Theato, P. *Biomacromolecules* **2010**, *11*, 2432–2439.
- (5) Aseyev, V.; Tenhu, H.; Winnik, F. In *Self Organized Nanostructures of Amphiphilic Block Copolymers II*; Müller, A. H. E., Borisov, O., Eds.; Springer: Berlin, 2011; Vol. 242, pp 29–89.
- (6) Liu, R.; Fraylich, M.; Saunders, B. *Colloid Polym. Sci.* **2009**, *287*, 627.
- (7) Büttin, V.; Liu, S.; Weaver, J. V. M.; Bories-Azeau, X.; Cai, Y.; Armes, S. P. *React. Funct. Polym.* **2006**, *66*, 157–165.
- (8) Principi, T.; Goh, C. C. E.; Liu, R. C. W.; Winnik, F. M. *Macromolecules* **2000**, *33*, 2958–2966.
- (9) Soga, O.; van Nostrum, C. F.; Hennink, W. E. *Biomacromolecules* **2004**, *5*, 818–821.
- (10) Sugihara, S.; Kanaoka, S.; Aoshima, S. *Macromolecules* **2004**, *37*, 1711–1719.
- (11) Zhu, X. X.; Avoce, D.; Liu, H. Y.; Benrebouh, A. *Macromol. Symp.* **2004**, *207*, 187–191.
- (12) Liu, H. Y.; Zhu, X. X. *Polymer* **1999**, *40*, 6985–6990.
- (13) Avoce, D.; Liu, H. Y.; Zhu, X. X. *Polymer* **2003**, *44*, 1081–1087.
- (14) Weiss, J.; Böttcher, C.; Laschewsky, A. *Soft Matter* **2011**, *7*, 483.
- (15) Lee, H.-N.; Bai, Z.; Newell, N.; Lodge, T. P. *Macromolecules* **2010**, *43*, 9522–9528.
- (16) Romão, R. I. S.; Beija, M.; Charreyre, M.-T. r. s.; Farinha, J. P. S.; Gonçalves da Silva, A. I. M. P. S.; Martinho, J. M. G. *Langmuir* **2009**, *26*, 1807–1815.
- (17) Maki, Y.; Mori, H.; Endo, T. *Macromol. Chem. Phys.* **2010**, *211*, 45–56.
- (18) Mertoglu, M.; Garnier, S.; Laschewsky, A.; Skrabania, K.; Storsberg, J. *Polymer* **2005**, *46*, 7726–7740.
- (19) Dimitrov, I.; Trzebicka, B.; Müller, A. H. E.; Dworak, A.; Tsvetanov, C. B. *Prog. Polym. Sci.* **2007**, *32*, 1275–1343.
- (20) Cao, Y.; Zhu, X. X.; Luo, J.; Liu, H. *Macromolecules* **2007**, *40*, 6481–6488.
- (21) Cao, Y.; Zhu, X. X. *Can. J. Chem.* **2007**, *85*, 407–411.
- (22) Cao, Y.; Zhao, N.; Wu, K.; Zhu, X. X. *Langmuir* **2009**, *25*, 1699–704.
- (23) Xie, D.; Ye, X.; Ding, Y.; Zhang, G.; Zhao, N.; Wu, K.; Cao, Y.; Zhu, X. X. *Macromolecules* **2009**, *42*, 2715–2720.
- (24) Braunecker, W. A.; Matyjaszewski, K. *Prog. Polym. Sci.* **2007**, *32*, 93–146.
- (25) Smith, A. E.; Xu, X.; McCormick, C. L. *Prog. Polym. Sci.* **2010**, *35*, 45–93.
- (26) Shea, K. J.; Stoddard, G. J.; Shavelle, D. M.; Wakui, F.; Choate, R. M. *Macromolecules* **1990**, *23*, 4497–4507.
- (27) Lai, J. T.; Filla, D.; Shea, R. *Macromolecules* **2002**, *35*, 6754–6756.
- (28) Idziak, I.; Avoce, D.; Lessard, D.; Gravel, D.; Zhu, X. X. *Macromolecules* **1999**, *32*, 1260–1263.
- (29) Boutris, C.; Chatzi, E. G.; Kiparissides, C. *Polymer* **1997**, *38*, 2567–2570.
- (30) de Lambert, B.; Charreyre, M.-T.; Chaix, C.; Pichot, C. *Polymer* **2005**, *46*, 623–637.
- (31) Schilli, C. M.; Zhang, M.; Rizzardo, E.; Thang, S. H.; Chong, Y. K.; Edwards, K.; Karlsson, G.; Müller, A. H. E. *Macromolecules* **2004**, *37*, 7861–7866.
- (32) Convertine, A. J.; Lokitz, B. S.; Lowe, A. B.; Scales, C. W.; Myrick, L. J.; McCormick, C. L. *Macromol. Rapid Commun.* **2005**, *26*, 791–795.
- (33) Favier, A.; Charreyre, M.-T.; Chaumont, P.; Pichot, C. *Macromolecules* **2002**, *35*, 8271–8280.
- (34) Lowe, A. B.; McCormick, C. L. *Prog. Polym. Sci.* **2007**, *32*, 283–351.
- (35) Sumerlin, B. S.; Donovan, M. S.; Mitsukami, Y.; Lowe, A. B.; McCormick, C. L. *Macromolecules* **2001**, *34*, 6561–6564.
- (36) Perrier, S.; Barner-Kowollik, C.; Quinn, J. F.; Vana, P.; Davis, T. P. *Macromolecules* **2002**, *35*, 8300–8306.
- (37) Yusa, S.-i.; Shimada, Y.; Mitsukami, Y.; Yamamoto, T.; Morishima, Y. *Macromolecules* **2004**, *37*, 7507–7513.
- (38) Stenzel, M. H. In *Handbook of RAFT Polymerization*; Barner-Kowollik, C., Ed.; Wiley-VCH Verlag GmbH: Weinheim, 2008; pp 315–372.
- (39) Kerker, M. In *The Scattering of Light, and Other Electromagnetic Radiation*; Academic Press: New York, 1969; p 339.
- (40) Lessard, D. G.; Ousale, M.; Zhu, X. X.; Eisenberg, A.; Carreau, P. J. *J. Polym. Sci., Part B: Polym. Phys.* **2003**, *41*, 1627–1637.
- (41) Wu, C.; Wang, X. *Phys. Rev. Lett.* **1998**, *80*, 4092–4094.
- (42) Wang, X.; Qiu, X.; Wu, C. *Macromolecules* **1998**, *31*, 2972–2976.
- (43) Weiss, J.; Laschewsky, A. *Langmuir* **2011**, *27*, 4465–4473.